Physics of the Dark Universe 30 (2020) 100660

Contents lists available at ScienceDirect

Physics of the Dark Universe

journal homepage: www.elsevier.com/locate/dark

Anti-de Sitter Hayward black holes in Einstein–Gauss–Bonnet gravity

Sushant G. Ghosh [a,b], Arun Kumar [a,*], Dharm Veer Singh [c]

[a] Centre for Theoretical Physics, Jamia Millia Islamia, New Delhi 110025, India
[b] Astrophysics and Cosmology Research Unit, School of Mathematics, Statistics and Computer Science, University of KwaZulu-Natal, Private Bag X54001, Durban 4000, South Africa
[c] Department of Physics, Institute of Applied Science and Humanities, GLA University, Matura 281406, India

ARTICLE INFO

Article history:
Received 30 March 2020
Received in revised form 18 June 2020
Accepted 29 June 2020

ABSTRACT

Lovelock gravitation theory is a natural extension of the General Relativity to higher dimensions with the inclusion of only second-order terms correspond to the Einstein–Gauss–Bonnet gravity. In this paper, we find an exact Hayward black hole solution of $D \geq 5$-dimensional spacetime for Einstein–Gauss–Bonnet (EGB) gravity with negative cosmological constant (Λ) minimally coupled to non-linear electrodynamics for a specific Lagrangian density, namely, EGB-AdS black holes, with additional parameter e because of magnetic charge. Interestingly, it turns out that for each value of GB parameter (α), there exist a critical e_E such that for $e < e_E$ describe non-extremal black holes with Cauchy (r_-) and Event horizons (r_+), while for $e = e_E$ corresponds to an extremal regular black hole with degenerate horizons ($r_+ = r_- = r_E$). Owing to the magnetically charged corrected black hole, the thermodynamic quantities have also been modified, but the entropy does not satisfy the usual area law. A divergence of the specific heat at $r_+ = r_c$, where the temperature attains maximum value and the Hawking–Page transition is achievable with the stable (unstable) branch for $r_{t1} \leq r_+ < r_c$ ($r_c < r_+ \leq r_{t2}$). Thus, we found Hayward EGB-AdS black holes which do not evaporate completely, but lead to stable double-horizon black hole remnants with vanishing temperature and positive heat capacity.

1. Introduction

The classical Einstein's gravity is the most reliable theory which predicts the existence of singularities inside black holes, and they are connected with the infinite growth of the curvature invariant. This is a well-known problem of the classical Einstein's theory of gravity, e.g., the black hole solutions, such as Schwarzschild and Reisner–Nordstrom, have curvature singularity at the center, which means spacetime fails to exist, signaling a breakdown of the physics laws at that point. However, there is a belief that these singularities are an artifact of General Relativity (GR) and do not exist in Nature. Thus, for these laws of physics to exist, singularities must be substituted by some other objects in a more suitable theory or the GR should be modified. While we were deprived of definite quantum gravity, which is expected to resolve singularity problem [1] and understand the interior of the black hole, and thus, attention was shifted to regular models (See, e.g., [2] for a review). The concept of a regular or singularity model started with the seminal Bardeen's paper [3], who proposed the first regular black hole which is solution of GR when coupled to nonlinear electrodynamics (NED) [4], yielding alteration to classical black holes, but near the center, they behave like a de Sitter spacetime. Subsequently, there has been intense activity for regular black holes that are exact solutions of the GR minimally coupled to NED [5–10].

A simple model of a regular (or non-singular) black hole was proposed by Hayward [11] which describes an isolated spherically symmetric regular spacetime given by the metric

$$ds^2 = -G(r)dt^2 + \frac{1}{G(r)}dr^2 + r^2(d\theta^2 + sin^2\theta d\phi^2), \tag{1}$$

with

$$G(r) = 1 - \frac{2Mr^2}{r^2 + 2l^2M}.$$

The Hayward black hole [11] can be derived using the following particular Lagrangian density [12,13]

$$\mathcal{L}(\mathcal{F}) = \frac{6}{se^2}\frac{(2e^2\mathcal{F})^{3/2}}{\left(1 + (2e^2\mathcal{F})^{3/4}\right)^2}, \tag{2}$$

where $s > 0$ is a constant, e is magnetic charge, M is a mass and $\mathcal{F}$ is $F_{\mu\nu}F^{\mu\nu}/4$. Here for convenience we write $e^3 = 2l^2M$. The Maxwell field tensor reads

$$F_{\mu\nu} = 2\delta^{\theta}_{[\mu}\delta^{\phi}_{\nu]}e(r)\sin\theta. \tag{3}$$

* Corresponding author.
E-mail addresses: sghosh2@jmi.ac.in (S.G. Ghosh), arunbidhan@gmail.com (A. Kumar), veerdsingh@gmail.com (D.V. Singh).

https://doi.org/10.1016/j.dark.2020.100660
2212-6864/

It turns out that the magnetic field strength $F_{\theta\,\phi} = e \sin\theta$, then $\mathcal{F}$ become

$$\mathcal{F} = \frac{e^2}{2r^4}, \tag{4}$$

where the magnetic charge e is defined as $\int \mathcal{F}/4\pi = e$. The Hayward solution (1) describes the spherically symmetric regular spacetime and mass M is the only parameter beside fundamental l, which determines the scale. At large distance $r \to \infty$, it gives Schwarzschild solution, while near origin ($r \to 0$), it has de Sitter form. Obviously, for $M > 3\sqrt{3}l/4$, the Hayward metric has the Cauchy (r_-) and the event horizon (r_+), corresponding to non-extremal black holes, while for $M_* = 3\sqrt{3}l/4$, $F(r)$ has double root $r_* = \sqrt{3}l$, corresponding to extremal Hayward black hole. The Hayward metric is simple for the analysis due to this scaling behavior [14]. It is also a simple exact model of general relativity minimally coupled to nonlinear electrodynamics (where charge e is related to M via $e^3 = 2Ml^2$) and hence was given significant attention [13,15].

It may be worth noting that the NED theories appear as low energy effective limits in some models of string/M-theory [16]. Further, the Einstein–Gauss–Bonnet (EGB) gravity been explored to a large extent due to its appearance in strings theories at low energies [17]. The EGB gravities are notably different from the general higher-curvature theories because of the field equations involving not more than second derivatives of the metric and thereby these are free from several problems that normally affect general higher derivative gravity theories. Also, such a theory may be used in the context of the AdS/CFT correspondence to investigate the effects of higher-curvature terms and allow us to explore several conceptual issues of black holes in-depth. Indeed, the general static spherically symmetric solution in EGB theory was discovered by Boulware and Deser [18] to show that the only stable solution has a Schwarzschild-type spacetime structure and the central singularity is still unpreventable which is true to the charged black holes [19]. The higher-curvature corrections to Einstein–Hilbert action make strong predictions about nature, the most important ones are the existence of higher dimensions [17]. Further, it is seen that within the framework of AdS/CFT correspondence, higher-derivative corrections to gravitational action in AdS space could lead to a modification in the dynamics of strongly coupled dual theory. This led to considerable activities in higher dimensions which are also motivated by the superstring and field theories. The black holes with higher derivative curvature in Anti-de Sitter (AdS) spaces have been considered in recent years, e.g., static AdS black hole solutions in EGB gravity with several interesting features [20–22]. Motivated by the above arguments in the context of AdS/CFT, we find Hayward-like regular black hole metrics for D-dimensional EGB gravity in AdS spacetimes, namely, Hayward EGB-AdS black holes. The metrics depend on the mass (M), coupling constant (α) and a charge parameter (e) coming from NED that measures the potential deviation from the Boulware–Deser black hole which is encompassed as a special case ($e = 0$). We also find exact expressions for the thermodynamical quantities associated with Hayward EGB-AdS black holes to find a stable black remnant and also perform a thermodynamic stability analysis.

2. Black hole solution in Einstein-Gauss–Bonnet gravity AdS spacetimes

Perhaps, one of the natural tools to investigate AdS/CFT is to examine higher curvature gravity AdS black holes and discuss their thermodynamics. Here we are interested in the Einstein–Gauss–Bonnet theory that is a generalization of general relativity with its action involving higher curvature corrections [23]. To begin with, we consider the D-dimensional action for EGB theory minimally coupled to nonlinear electrodynamics [24]

$$\mathcal{I}_G = \frac{1}{2\kappa_D^2}\int_{\mathcal{M}} d^Dx\sqrt{-g}\left[R + \alpha(R^2 - 4R_{\mu\nu}R^{\mu\nu} + R_{\mu\nu\gamma\delta}R^{\mu\nu\gamma\delta}) \right.$$
$$\left. -2\Lambda + \mathcal{L}(F)\right], \tag{5}$$

where, the negative cosmological constant $\Lambda = -(D-1)(D-2)/2l^2$, $\kappa_D = \sqrt{8\pi G_D}$ with D-dimensional gravitational constant G_D and α is the Gauss–Bonnet coupling coefficient with dimension $(length)^2$. In the heterotic string theory, α is positive, hence we keep the discussion restricted to the case $\alpha \geq 0$ [18]. In $D \geq 5$ dimensions, the Gauss–Bonnet term gives non-trivial modification to the dynamics of gravity. By varying the action with respect to the metric $g_{\mu\nu}$, we get the following Einstein–Gauss–Bonnet equations of motion

$$G^E_{\mu\nu} + \alpha H_{\mu\nu} + \Lambda g_{\mu\nu} = T_{\mu\nu} \equiv 2\left[\frac{\partial\mathcal{L}(F)}{\partial F}F_{\mu\rho}F^{\rho}_{\nu} - g_{\mu\nu}\mathcal{L}(F)\right], \tag{6}$$

and the tensor $F_{\mu\nu}$ obeys the dynamic equation

$$\nabla_\mu\left(\frac{\partial\mathcal{L}(F)}{\partial F}F_{\mu\nu}\right) = 0 \tag{7}$$

and the Bianchi identities

$$\nabla_\mu\left({}^*F_{\mu\nu}\right) = 0, \tag{8}$$

where $*$ denotes the Hodge dual. $G_{\mu\nu}$ and $H_{\mu\nu}$, respectively, read [25]

$$G_{\mu\nu} = R_{\mu\nu} - \frac{1}{2}g_{\mu\nu}R,$$
$$H_{\mu\nu} = 2\left(-R_{\mu\sigma\kappa\tau}R^{\kappa\tau\sigma}{}_{\nu} - 2R_{\mu\rho\nu\sigma}R^{\rho\sigma} - 2R_{\mu\sigma}R^{\sigma}{}_{\nu} + RR_{\mu\nu}\right)$$
$$-\frac{1}{2}\mathcal{L}_{GB}g_{\mu\nu}, \tag{9}$$

where $G_{\mu\nu}$ is the Einstein tensor, $H_{\mu\nu}$ is the Lanczos tensor and $T_{\mu\nu}$ is energy–momentum tensor. Here, we are interested in D-dimensional static spherically symmetric solutions in the theory described by the action (5) with the metric *ansatz* [26]

$$ds^2 = -f(r)dt^2 + \frac{1}{f(r)}dr^2 + r^2\tilde{\gamma}_{ij}\,dx^i\,dx^j, \tag{10}$$

where $\tilde{\gamma}_{ij}$ is the metric of a (D-2)-dimensional constant curvature space $k = 1,\ 0,$ or -1 and $f(r)$ is the metric function to be determined, but we shall restrict to $k = 1$.

The Maxwell field tensor in $D \geq 5$ reads [27]

$$F_{\mu\nu} = 2\delta^{\theta_{D-3}}_{[\mu}\delta^{\theta_{D-2}}_{\nu]}\frac{e(r)^{D-3}}{r^{D-4}}\sin\theta_{D-3}\left[\prod_{j=1}^{D-4}\sin^2\theta_j\right], \tag{11}$$

with $\mathcal{F}$ as

$$\mathcal{F} = \frac{e^2(D-3)}{2r^2(D-2)} \tag{12}$$

From Eq. (7), one can see that $dF = 0$, using that we get

$$e'(r)2\delta^{\theta_{D-3}}_{[\mu}\delta^{\theta_{D-2}}_{\nu]}\frac{e(r)^{D-3}}{r^{D-4}}\sin\theta_{D-3}\left[\prod_{j=1}^{D-4}\sin^2\theta_j\right]$$
$$\times\ d\theta\wedge d\phi\wedge\ldots\wedge d\psi_{(D-2)} = 0. \tag{13}$$

This leads to $e(r) = e =$ constant. Interestingly, influence of the other component of $F_{\mu\nu}$ is negligible compared to $F_{\theta\phi}$ [28]. In order to get regular black holes, we modify the Lagrangian density to D-dimensional spacetimes as [29]

$$\mathcal{L}(F) = \frac{(D-1)(2e^2F)^{\frac{D-1}{D-2}}}{2se^2(1+(\sqrt{2eF})^{\frac{D-1}{D-2}})} \quad \text{with} \quad s = \frac{e^{D-3}}{(D-2)\mu'}. \tag{14}$$

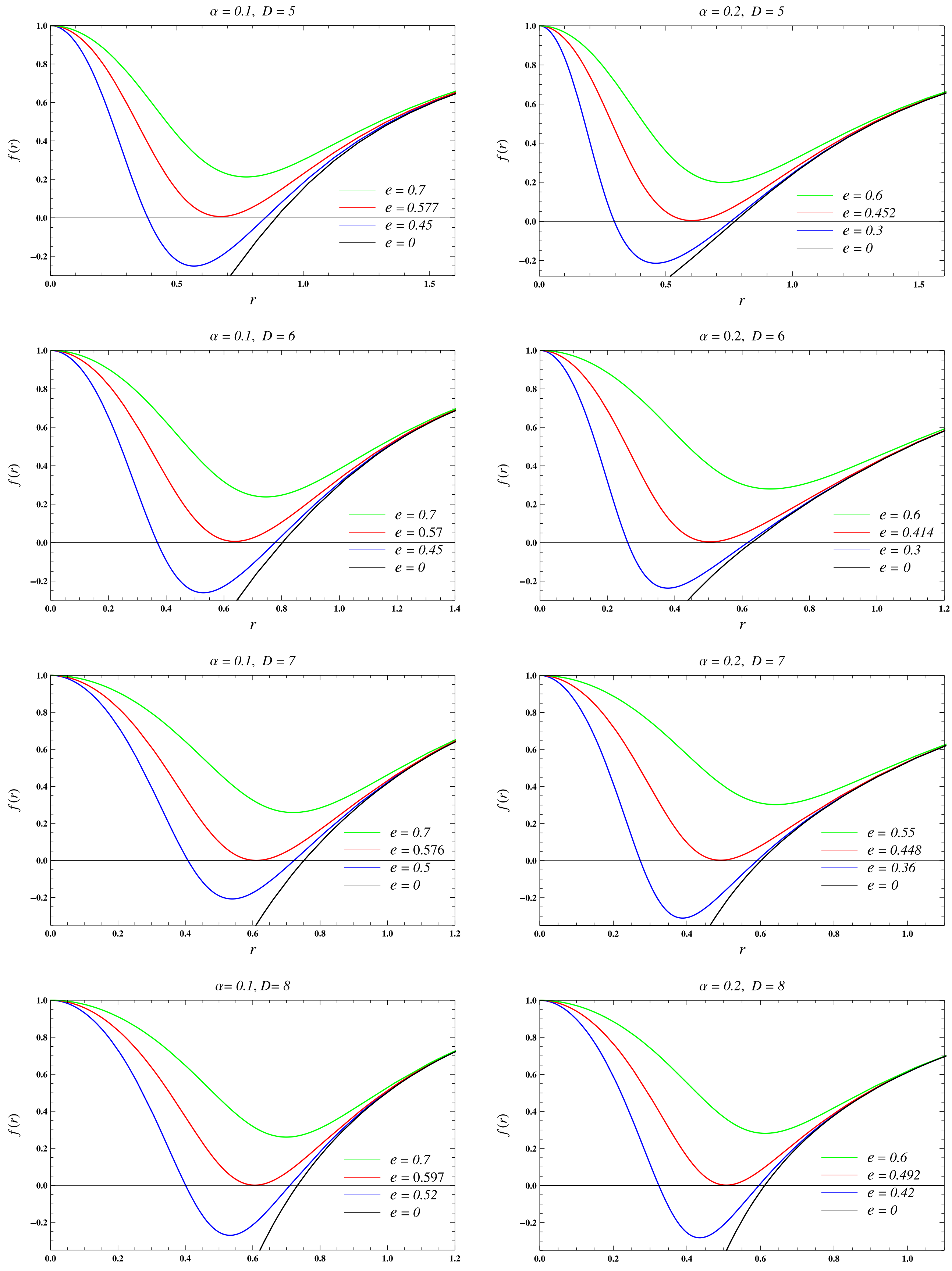

Fig. 1. The horizons of Hayward EGB-AdS black holes in various dimensions $D = 5$, 6, 7, and 8 (top to bottom) for different values of e with $e = 0$ corresponds to EGB-AdS black holes.

Substituting Eq. (12) in Eq. (14), one obtains

$$\mathcal{L}(F)=\frac{(D-1)(D-2)\mu' e^{D-1}}{2(r^{D-1}+e^{D-1})^2} \tag{15}$$

The Gauss–Bonnet gravity square term in the action (5) is the only contribution for which action is free from ghosts [30]. Using metric (10), we obtain the (r,r) field equation is given by

$$(D-2)\Big[\Big(r^3-2\tilde{\alpha}r\,(f\,(r)-1)\Big)f'\,(r)+(D-3)\,r^2\,(f\,(r)-1)$$
$$(D-5)\,\tilde{\alpha}\,(f\,(r)-1)^2\Big]+\Lambda=\frac{(D-1)(D-2)\mu' e^{D-1}}{(r^{D-1}+e^{D-1})^2}, \tag{16}$$

where a prime ($'$) denotes a derivative with respect to r and $\tilde{\alpha}=(D-3)\,(D-4)\,\alpha$. Eq. (16) admits the following solution

$$f_{\pm}\,(r)=1+\frac{r^2}{2\tilde{\alpha}}\left(1\pm\sqrt{1+\frac{4\tilde{\alpha}\mu'}{r^{D-1}+e^{D-1}}-\frac{4\tilde{\alpha}}{l^2}}\right),\qquad D\geq 5 \tag{17}$$

where the mass term μ' is a constant of integration and is related to the mass M of the black hole via

$$\mu'=\frac{16\pi M}{(D-2)V_{D-2}},\quad V_{D-2}=\frac{2\pi^{(D-1)/2}}{\Gamma(D-1)/2}, \tag{18}$$

where V_{D-2} is the volume of the $(D-2)$-dimensional unit sphere. The $(\pm)$ sign in front of square root in (17) corresponds to two different branches of the solution [26]. It seen that the (17) satisfy all field equations. The well known Boulware–Deser solution [18] is encompassed as a special case in the absence of NED ($e=0$). The negative branch of (17), in general relativity limit $\alpha\to 0$, leads

$$f_{-}(r)\approx 1-\frac{\mu' r^2}{r^{D-1}+e^{D-1}}+\frac{r^2}{l^2}, \tag{19}$$

which is D-dimensional Hayward AdS solution [14]. Further, if we switch off the charge ($e=0$) the solution simplifies to

$$f_{-}(r)\approx 1-\frac{\mu'}{r^{D-3}}+\frac{r^2}{l^2}. \tag{20}$$

Hence, the negative branch leads to a D-dimensional Schwarzschild–Tangherlini AdS black holes [31]. Thus, the negative branch of the solution (17) leads to all correct solutions in general relativity limits, and henceforth we shall restrict to only the negative branch of the solution, $f(r)\equiv f_{-}(r)$. For definiteness, henceforth, the solution (17) will be called Hayward EGB-AdS black holes. The Hayward EGB-AdS black hole, when ($\mu'=0$), reduces to

$$f(r)=1+\frac{r^2}{l^2_{eff}}\quad\text{with}\quad\frac{1}{l^2_{eff}}=\frac{1}{2\tilde{\alpha}}(1-\sqrt{1-\frac{4\tilde{\alpha}}{l^2}}) \tag{21}$$

and also near the origin it behaves like de Sitter as

$$f(r)=1+\frac{r^2}{l^2_{eff}}\quad\text{with}\quad\frac{1}{l^2_{eff}}=\frac{1}{2\tilde{\alpha}}(1-\sqrt{1+\frac{4\mu'\tilde{\alpha}}{e^{D-1}}-\frac{4\tilde{\alpha}}{l^2}}). \tag{22}$$

Note that the AdS curvature radius l^2 is related to cosmological constant Λ and $l^2>0$ for $\Lambda<0$.

The behavior of invariants like, Ricci scalar (R), Ricci square ($\mathcal{R}=R_{ab}R^{ab}$) and Kretschmann scalar ($\mathcal{K}=R_{abcd}R^{abcd}$) is useful to address the singularity. These invariants for Hayward EGB-AdS black hole solution, respectively, read as given below

$$\lim_{r\to 0}R=\frac{D(D-1)}{2\tilde{\alpha}}\left[-1+\left(1+\frac{4\mu'\tilde{\alpha}}{e^{D-1}}-\frac{4\tilde{\alpha}}{l^2}\right)^{1/2}\right],$$

$$\lim_{r\to 0}\mathcal{R}=\frac{D(D-1)^2}{2\tilde{\alpha}^2}\left[1+\frac{2\mu'\tilde{\alpha}}{e^{D-1}}-\frac{2\tilde{\alpha}}{l^2}-\left(1+\frac{4\mu'\tilde{\alpha}}{e^{D-1}}-\frac{4\tilde{\alpha}}{l^2}\right)^{1/2}\right],$$

$$\lim_{r\to 0}\mathcal{K}=\frac{D(D-1)}{\tilde{\alpha}^2}\left[1+\frac{2\mu'\tilde{\alpha}}{e^{D-1}}-\frac{2\tilde{\alpha}}{l^2}-\left(1+\frac{4\mu'\tilde{\alpha}}{e^{D-1}}-\frac{4\tilde{\alpha}}{l^2}\right)^{1/2}\right]. \tag{23}$$

From the expression of invariants (23), we conclude that all of these invariants are finite and regular everywhere including at the origin ($r=0$) and the Hayward EGB-AdS spacetime is regular everywhere. Thus, we have seen that EGB coupled to NED with $L(F)$ defined in (14) leads to exact Hayward-like regular solution in D-dimensional AdS spacetimes.

We shall now discuss the horizon structure of Hayward EGB-AdS black holes. The metric (10) is singular at $f(r)=0$, signaling the existence of horizons. Thus, the radii of the horizons are the zeros of

$$r^{D-3}+\tilde{\alpha}r^{D-5}+\frac{r^{D-1}}{l^2}-\mu'-e^{D-1}(\frac{1}{l^2}+\frac{1}{r^2}+\frac{\tilde{\alpha}}{r^4})=0. \tag{24}$$

One can recover, in the absence of NED, the results [22]

$$r^{D-3}+\tilde{\alpha}r^{D-5}+\frac{r^{D-1}}{l^2}-\mu'=0, \tag{25}$$

which further reduces to the results obtained in [32] when $l^2\to\infty$ or ($\Lambda\to 0$). The horizon for EGB-AdS ($D=5$) black holes [22], is given by

$$r_+^2=\frac{l^2}{2}\left[-1+\sqrt{1+\frac{4(M-\tilde{\alpha})}{l^2}}\right] \tag{26}$$

We notice that there exists an extremal value of charge $e=e_E$ such that for $e<e_E$, the black holes have two horizon radii $r_{\pm}$ (cf. Fig. 1) with Cauchy horizon (r_-) and the event horizon (r_+). For $e=e_E$, the horizons degenerate to $r_e=r_{\pm}$, the horizon radius of extremal black hole, and, if charge $e>e_E$, then no black hole will exist. The Cauchy and event horizon radii are summarized in Table 1, for different values of e and α in various dimensions. From Table 1, one can notice radius of Cauchy horizon increases, whereas the event horizon radius decreases when we increase the value of e and α. These radii show the same trend as we go to the higher dimensions.

3. Black hole thermodynamics

It was first shown by Wheeler [33,34] that any system consists of a black hole violates the non-decreasing entropy law, which makes it necessary to assign temperature and entropy to a black hole. Particularly, the thermodynamics of AdS black holes has been of great interest to the astrophysicists since the pioneering work by Hawking and Page, which suggested the existence of a phase transition in AdS black holes [35]. Having found the solution (17), we can turn our attention to the thermodynamics of black holes. The mass of the black holes, in terms of horizon radius r_+, are determined by using $f(r_+)=0$, which reads

$$M_+=\frac{(D-2)V_{D-2}\,r_+^{D-3}}{16\pi}\left[(1+\frac{\tilde{\alpha}}{r_+^2}+\frac{r_+^2}{l^2})(1+\frac{e^{D-1}}{r_+^{D-1}})\right]. \tag{27}$$

This shows that the mass term has been corrected due to GB term, NED and cosmological constant. In the limit $e=0$, we get

$$M_+^{EGB-AdS}=\frac{(D-2)V_{D-2}\,r_+^{D-3}}{16\pi}\left[1+\frac{\tilde{\alpha}}{r_+^2}+\frac{r_+^2}{l^2}\right]. \tag{28}$$

and one recovers the results of EGB-AdS black holes [22,26,27,36]. Further reduces to mass of the Gauss–Bonnet black holes [26,27] when $1/l^2=0$

$$M_+^{EGB}=\frac{(D-2)V_{D-2}\,r_+^{D-3}}{16\pi}\left[1+\frac{\tilde{\alpha}}{r_+^2}\right]. \tag{29}$$

Table 1
Cauchy horizon radius (r_-), the event horizon radius (r_+) and $\delta = r_+ - r_-$ for different values of charge e.

Dimensions	$\alpha = 0.1$				$\alpha = 0.2$			
	e	r_-	r_+	δ	e	r_-	r_+	δ
$D = 5$	0.2	0.1460	0.8894	0.7434	0.2	0.1873	0.7797	0.5924
	0.3	0.2286	0.8836	0.6550	0.3	0.2962	0.7672	0.4710
	$e_E = 0.577$	0.6821	0.6821	0	$e_E = 0.452$	0.6051	0.6051	0
$D = 6$	0.2	0.1207	0.8014	0.6807	0.2	0.1477	0.6256	0.4779
	0.3	0.2059	0.7989	0.5930	0.3	0.2604	0.6157	0.3553
	$e_E = 0.57$	0.6821	0.6821	0	$e_E = 0.414$	0.5041	0.5041	0
$D = 7$	0.2	0.0940	0.7518	0.6578	0.2	0.1123	0.6012	0.4889
	0.3	0.1747	0.7507	0.5760	0.3	0.2115	0.5973	0.3858
	$e_E = 0.576$	0.6187	0.6187	0	$e_E = 0.448$	0.4941	0.4941	0
$D = 8$	0.2	0.0711	0.7328	0.6617	0.2	0.0846	0.6113	0.5267
	0.3	0.1452	0.7325	0.5873	0.3	0.1732	0.6100	0.4368
	$e_E = 0.597$	0.6087	0.6087	0	$e_E = 0.492$	0.5055	0.5055	0

For the case $\alpha \to 0$, $1/l^2 = 0$, we get the mass for D-dimensional Hayward black holes

$$M_+^H = \frac{(D-2)V_{D-2}\, r_+^{D-3}}{16\pi}\left[1 + \frac{e^{D-1}}{r_+^{D-1}}\right], \tag{30}$$

which further reduces to the mass of well known Schwarzschild–Tangherlini black holes [26,37,38], when we choose $e = 0$ in (30). The temperature of the black hole horizon is related by the periodicity in the imaginary time of the metric. The Hawking temperature of the black hole as in the GR case is simply $T = \kappa/2\pi$ [22,32], where κ is the surface gravity defined by

$$\kappa^2 = -\frac{1}{2}\nabla_\mu \xi_\nu \nabla^\mu \xi^\nu, \tag{31}$$

where, ξ^μ is a Killing vector. For static spherically symmetric case the Killing vector ξ^μ, takes the form $\xi^\mu = \partial_t^\mu$. Thus, the Hawking temperature of the Hayward EGB-AdS black holes reads

$$T_+ = \frac{(D-3)}{4\pi r_+}\left[\frac{r_+^2 + \frac{(D-5)}{(D-3)}\tilde{\alpha} - \frac{2}{(D-3)}\frac{e^{D-1}}{r_+^{D-1}}(r_+^2 + 2\tilde{\alpha}) + \frac{(D-1)}{(D-3)l^2}r_+^4}{(r_+^2 + 2\tilde{\alpha})(1 + \frac{e^{D-1}}{r_+^{D-1}})}\right]. \tag{32}$$

Note that charge e and cosmological constant $1/l^2$ in Eq. (32) modifies the Gauss–Bonnet black hole [39] temperature. In Fig. 2, we have plotted the Hawking temperature as a function of horizon radius r_+ when $D = 5, 6, 7$ and 8. From Fig. 2 and Table 2 we noticed that the peaks of Hawking temperature decrease and shift toward the right as the value of magnetic charge (e) grows for a given value of the Gauss–Bonnet coupling parameter (α) and cosmological constant ($1/l^2$). It is also noteworthy that the temperature for EGB-AdS black holes diverges in $D > 5$ spacetime dimensions. Fig. 3 is showing that the temperature of Hayward black holes remains finite, but on the other hand, it diverges for the Schwarzschild–Tangherlini black holes. When, $e = 0$, Eq. (32) simplifies to [22,26,36,40]

$$T_+^{EGB-AdS} = \frac{(D-3)}{4\pi r_+}\left[\frac{r_+^2 + \frac{(D-5)}{(D-3)}\tilde{\alpha} + \frac{(D-1)}{(D-3)l^2}r_+^4}{r_+^2 + 2\tilde{\alpha}}\right], \tag{33}$$

and taking the limit $e = 1/l^2 = 0$, we recover the EGB black holes [26,27,32] temperature which reads

$$T_+^{EGB} = \frac{(D-3)}{4\pi r_+}\left[\frac{r_+^2 + \frac{(D-5)}{(D-3)}\tilde{\alpha}}{r_+^2 + 2\tilde{\alpha}}\right] \tag{34}$$

Table 2
The maximum Hawking temperature T_+^{Max} at critical radius r_c^T for different values of charge e and different dimension $D = 5, 6, 7$ and 8.

Dimensions	$\alpha = 0.1$			$\alpha = 0.2$		
	e	r_c^T	T_+^{Max}	e	r_c^T	T_+^{Max}
$D = 5$	0.2	0.6839	0.1216	0.2	0.8964	0.0868
	0.3	0.7927	0.1146	0.3	0.9715	0.0847
	0.577	1.1681	0.0890	0.452	1.1429	0.0787
$D = 6$	0.2	0.4644	0.1434	0.2	0.4239	0.1149
	0.3	0.7237	0.1333	0.3	0.7046	0.0998
	0.57	1.1432	0.1153	0.414	0.9888	0.0940
$D = 7$	0.2	0.3368	0.2370	0.2	0.3319	0.2222
	0.3	0.5220	0.1813	0.3	0.5068	0.1604
	0.576	1.0450	0.1378	0.448	0.7829	0.1242
$D = 8$	0.2	0.3023	0.3658	0.2	0.3007	0.3563
	0.3	0.4592	0.2594	0.3	0.4540	0.2454
	0.597	0.9541	0.1657	0.492	0.7581	0.1721

and when $\alpha = 1/l^2 = 0$, it takes the form of Hayward black holes temperature in D-dimensions

$$T_+^H = \frac{(D-3)}{4\pi r_+}\left[\frac{1 - \frac{2}{(D-3)}\frac{e^{D-1}}{r_+^{D-1}}}{1 + \frac{e^{D-1}}{r_+^{D-1}}}\right], \tag{35}$$

which further reduces to Schwarzschild–Tangherlini black holes [26,27,37] temperature, $T_+ = (D-3)/4\pi r_+$, when we take $e = 0$ in (35).

To find the entropy associated with Hayward EGB-AdS black holes, we use the first law of thermodynamics [22,26,27]

$$dM_+ = T_+ dS_+ + \Phi de, \tag{36}$$

Now, substituting Eqs. (27) and (32) in Eq. (36) and integrating with constant e, we obtained the entropy of Hayward EGB-AdS black holes

$$S_+ = \frac{V_{D-2}r_+^{D-2}}{4}\left[1 + 2\frac{(D-2)}{(D-4)}\frac{\tilde{\alpha}}{r_+^2} - (D-2)\frac{e^{D-1}}{r_+^{D-1}}\left(1 + \frac{2}{3}\frac{\tilde{\alpha}}{r_+^2}\right)\right]. \tag{37}$$

The terms in the parenthesis modify the entropy, and area law is not obeyed [41]. Since $\tilde{\alpha} > 0$, the entropy of both Hayward EGB-AdS and EGB-AdS ($e = 0$) black holes increase in all dimensions D (Fig. 4). The entropy of Hayward EGB-AdS black holes is independent of $1/l^2$, so the expression of entropy for both, EGB and EGB-AdS black holes is same, which can be obtained by switching off charge ($e = 0$) off as

$$S_+^{EGB} = \frac{V_{D-2}r_+^{D-2}}{4}\left[1 + 2\frac{(D-2)}{(D-4)}\frac{\tilde{\alpha}}{r_+^2}\right], \tag{38}$$

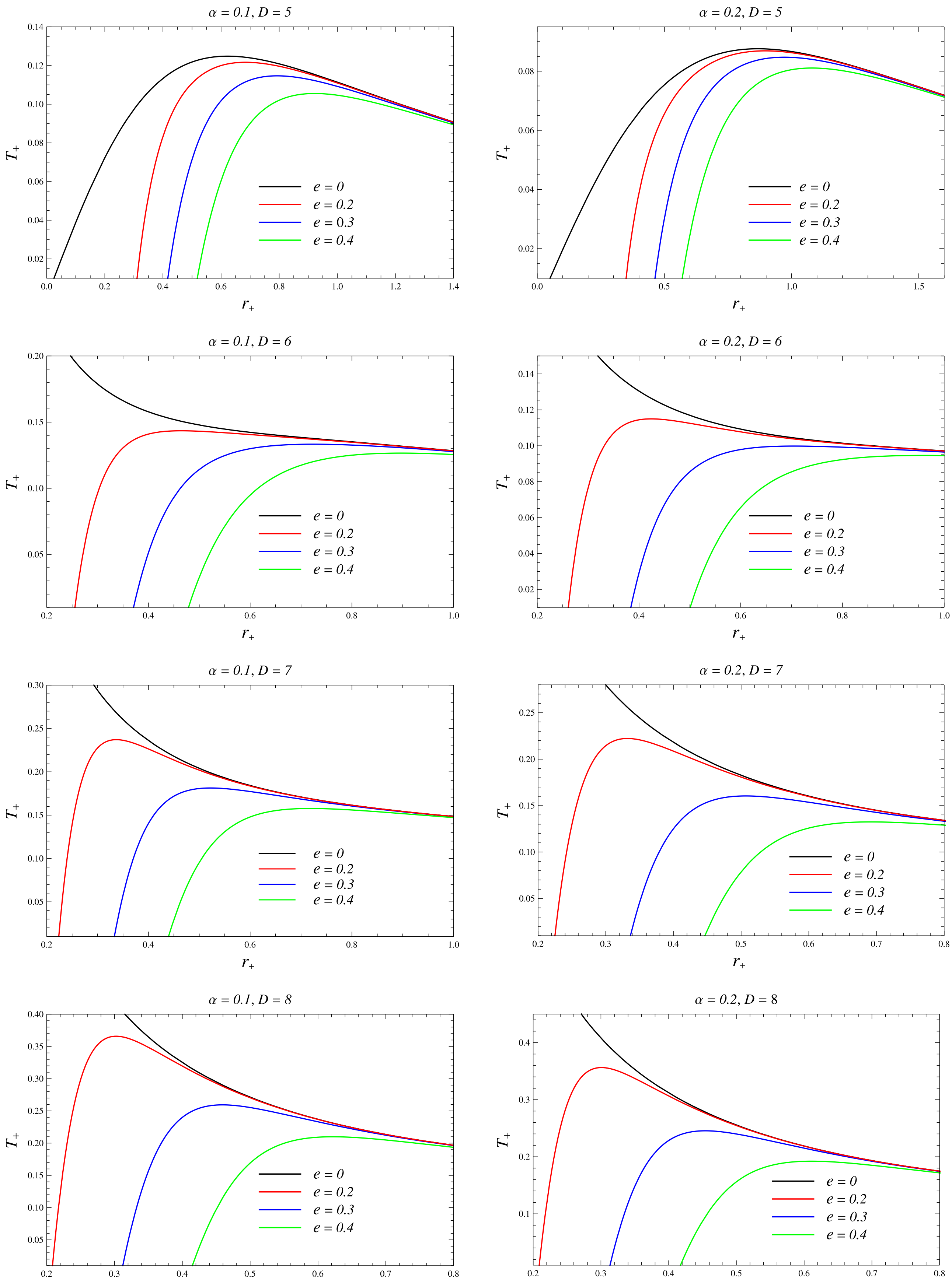

Fig. 2. Hayward EGB-AdS black holes temperature T_+ vs. horizon radius r_+ in various dimensions $D = 5$, 6, 7, and 8 (top to bottom) for different values of e with $e = 0$ corresponds to EGB-AdS black holes.

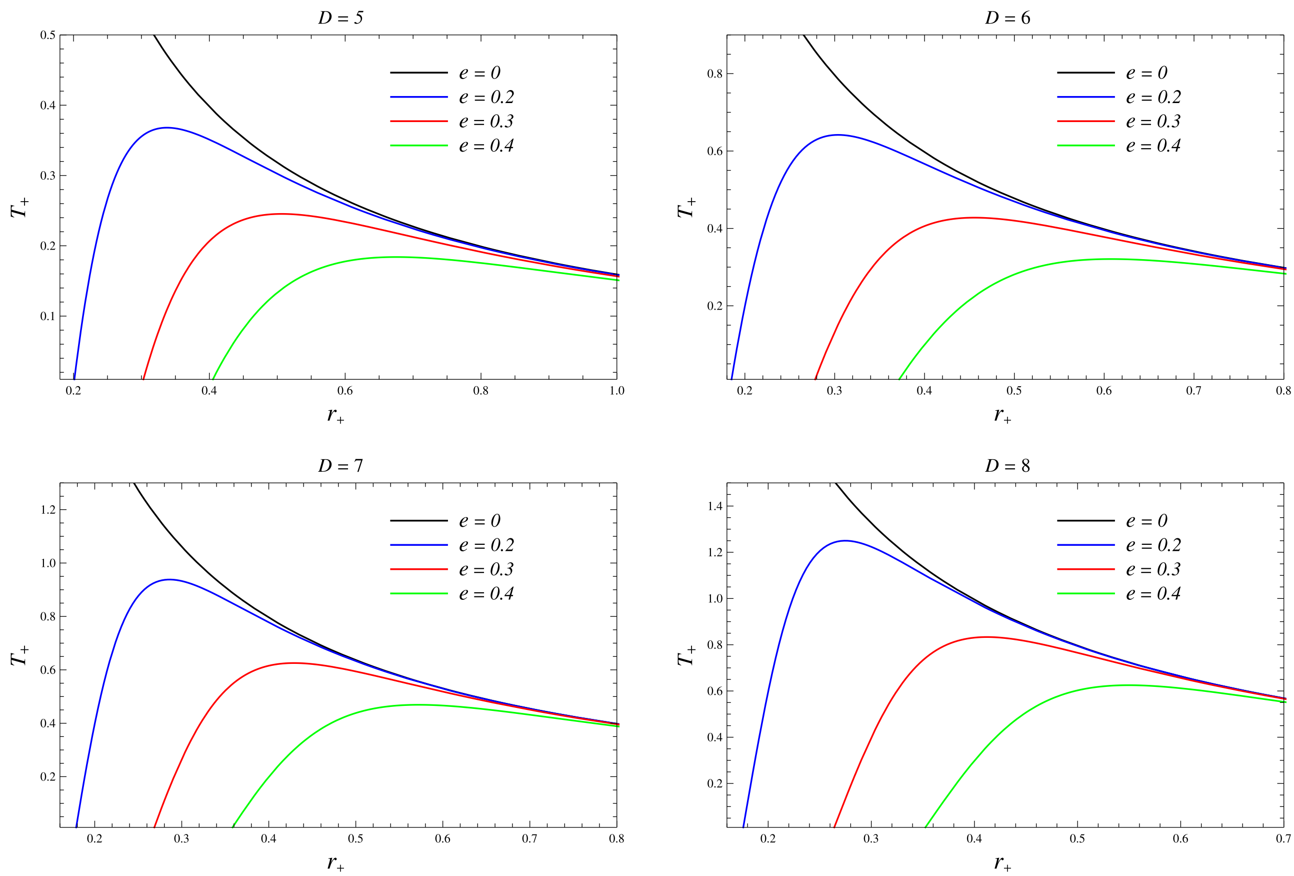

Fig. 3. Hayward black holes temperature T_+ vs. horizon radius r_+ in various dimensions $D = 5$, 6, 7, and 8 for different values of e with $e = 0$ corresponds to Schwarzschild–Tangherlini black holes.

which is exactly obtained previously [22,26,27,32,36]. Further, in the limit $\alpha = 0$, it reduces to the entropy of D-dimensional Hayward black holes

$$S_+^H = \frac{V_{D-2} r_+^{D-2}}{4}\left[1-(D-2)\frac{e^{D-1}}{r_+^{D-1}}\right]. \tag{39}$$

For the limiting case, $e = \alpha = 0$ and $1/l^2 = 0$, we get the entropy for Schwarzschild–Tangherlini black holes [26,27], as $S = A/4$, where $A = V_{D-2} r_+^{D-2}$ is the area of horizon in D-dimensions and thereby area law is restored.

The thermodynamic stability of a black hole is performed by analyzing the behavior of its specific heat [26,27]. The specific heat of a black hole is defined by

$$C_+ = \frac{\partial M_+}{\partial T_+} = \left(\frac{\partial M_+}{\partial r_+}\right)\left(\frac{\partial r_+}{\partial T_+}\right). \tag{40}$$

Using Eqs. (40), (27), and (32), we get the heat capacity of Hayward EGB-AdS black holes

$$\begin{aligned} C_+ = \frac{(D-2)(D-3)V_{D-2}}{\beta} r_+^{D-4}\Bigg[&\left(1+\frac{e^{D-1}}{r_+^{D-1}}\right)^2 (r_+^2+2\tilde{\alpha})^2 \\ &\times\left(r_+^2+\frac{D-5}{D-3}\tilde{\alpha}-\frac{2}{D-3}\frac{e^{D-1}}{r_+^{D-1}}(r_+^2+2\tilde{\alpha}) \right.\\ &\left.+\frac{D-1}{(D-3)l^2}r_+^4\right)\Bigg], \end{aligned} \tag{41}$$

with

$$\begin{aligned} \beta = 4\Bigg[& 2(r_+^2+2\tilde{\alpha})^2\left(\frac{e^{D-1}}{r_+^{D-1}}\right)^2 + \Bigg((D^2-3D+6)r_+^4+\frac{D(D-1)}{l^2}r_+^6 \\ &+\left((3D^2-7D+20)r_+^2+\frac{2(D-1)(D-2)}{l^2}r_+^4\right)\tilde{\alpha} \\ &+2(D^2-3D+10)\tilde{\alpha}^2\Bigg)\frac{e^{D-1}}{r_+^{D-1}} \\ &+\left(\frac{D-1}{l^2}r_+^2-D+3\right)r_+^4+\left(\frac{6(D-1)}{l^2}r_+^4-(D-9)r_+^2\right)\tilde{\alpha} \\ &-2(D-5)\tilde{\alpha}^2\Bigg] \end{aligned}$$

The behavior of specific heat of Hayward EGB-AdS and Hayward black holes, respectively, has been depicted in Figs. 5–7. The regions with $C_+ > 0(< 0)$, are the regions in which the black holes are thermodynamically stable (unstable). From Fig. 5, the specific heat C_+ of Hayward EGB-AdS black holes diverges at a critical horizon radius say r_c, confirming the existence of the second order phase transition [35]. The Hayward EGB-AdS black holes in the regions $r_{t1} < r_+ < r_c$ and $r_+ > r_{t2}$ are thermodynamically stable, whereas the black holes are thermodynamically unstable when $r_+ > r_{t1}$ and $r_c < r_+ < r_{t2}$, but, Hayward black holes are thermodynamically stable only in the region $r_t \le r_+ \le r_{c1}$ and unstable in the regions $r_+ < r_t$ and $r_+ > r_{c1}$ (cf. Fig. 7). It is important to note that there exists multiple transition for Hayward EGB-AdS black holes (Figs. 5 and 6). Here, we can also notice that the value of critical radius r_c increases we increase with the value of either e or α. On the other hand, value of r_c decreases with D. The regions of thermodynamical stability are summarized in Table 3, out of which two are representing thermodynamically stable black holes and remaining two regions are representing thermodynamically unstable black holes. In the absence of magnetic charge (e), we reduce to the expression for

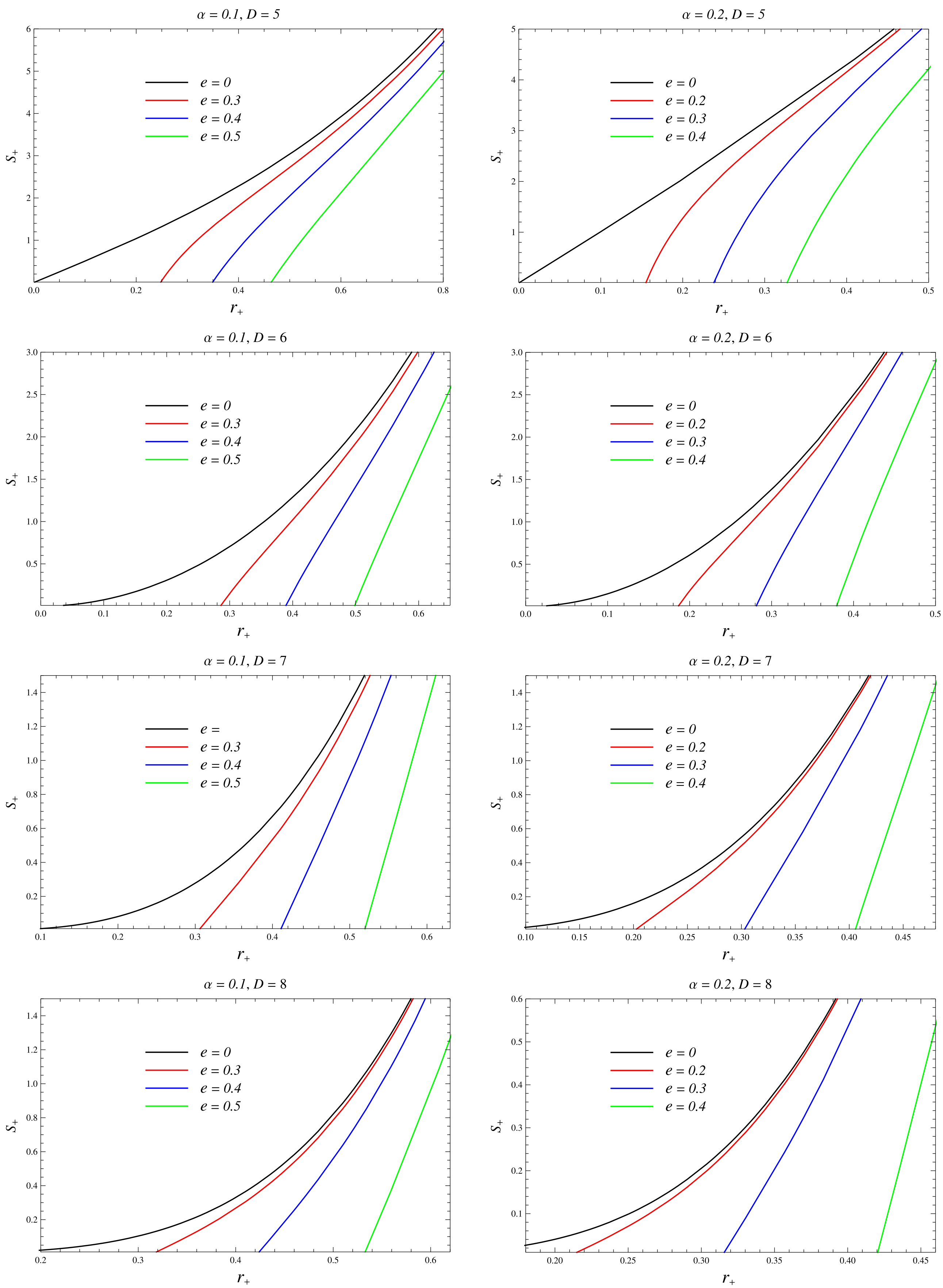

Fig. 4. Hayward EGB-AdS black holes entropy S_+ vs. horizon radius r_+ in various dimensions $D = 5$, 6, 7, and 8 (top to bottom) for different values of e with $e = 0$ corresponds to EGB-AdS black holes.

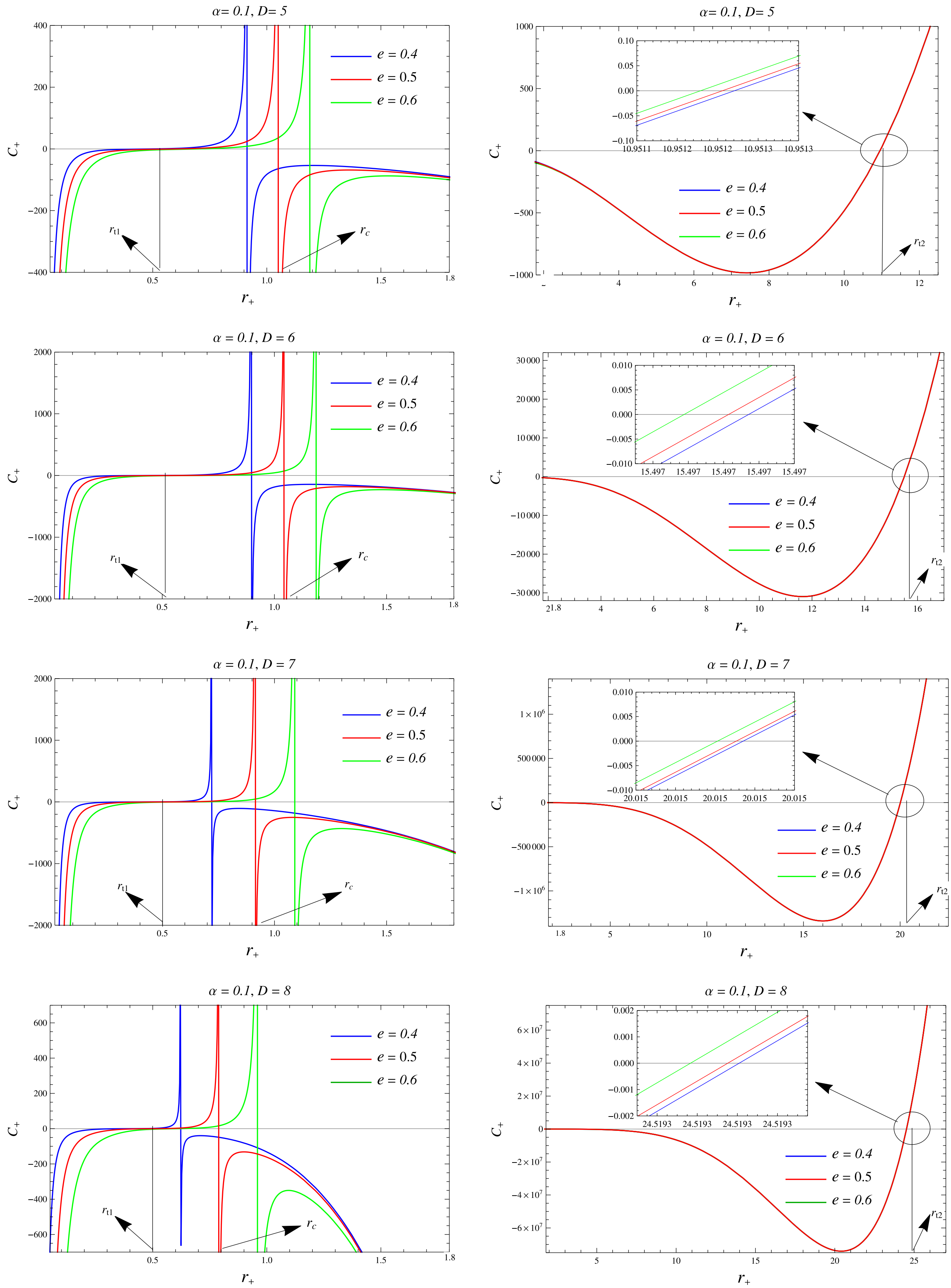

Fig. 5. Hayward EGB-AdS black holes specific heat C_+ vs. horizon radius r_+ (left($0 \leq r_+ \leq 1.8$ and right ($r_+ \geq 1.8$)) in various dimensions $D = 5$, 6, 7, and 8 (top to bottom) for different values of e.

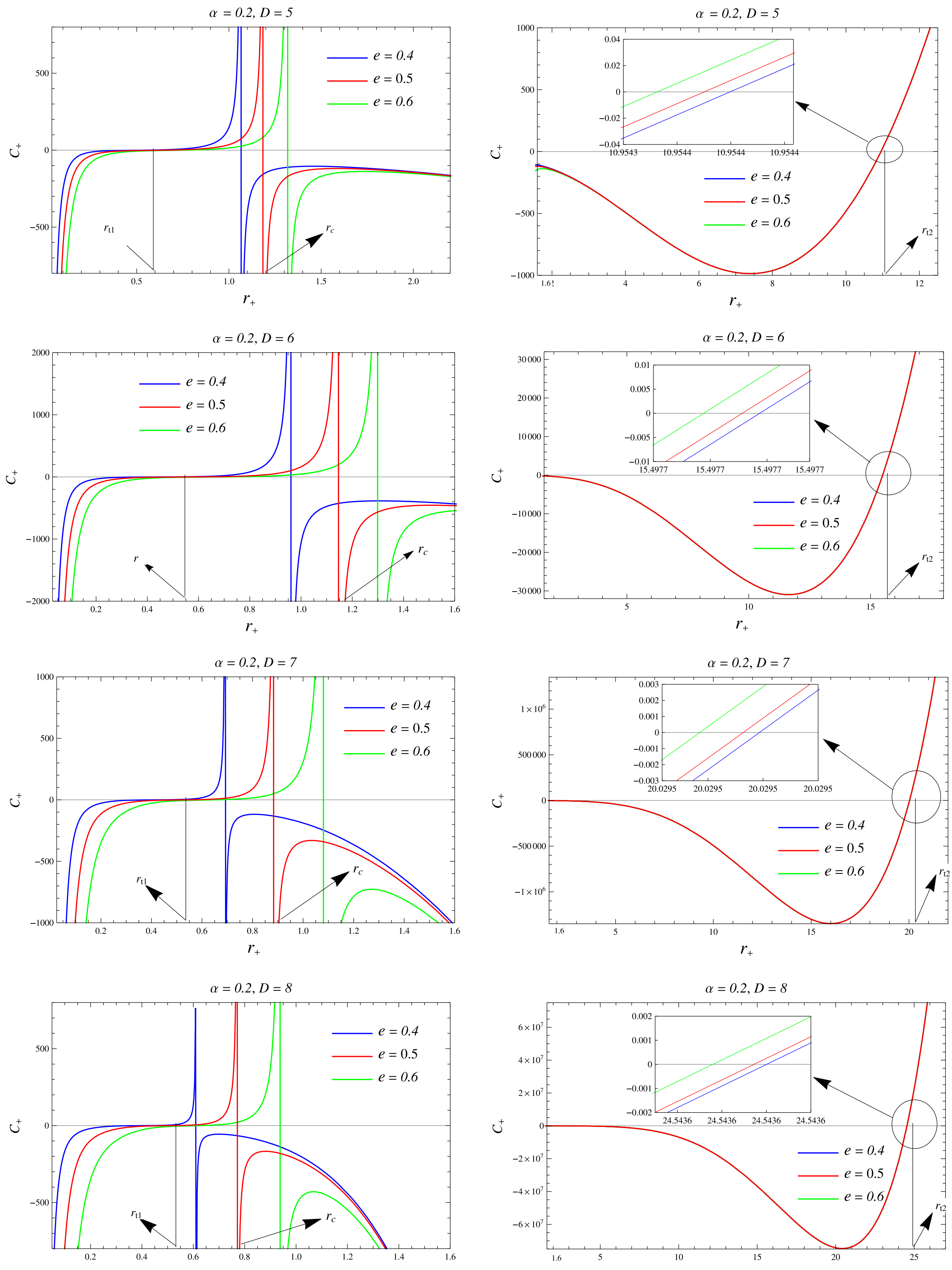

Fig. 6. Hayward EGB-AdS black holes specific heat C_+ vs. horizon radius r_+ (left($0 \leq r_+ \leq 1.6$ and right ($r_+ \geq 1.6$)) in various dimensions $D = 5, 6, 7$, and 8 (top to bottom) for different values of e.

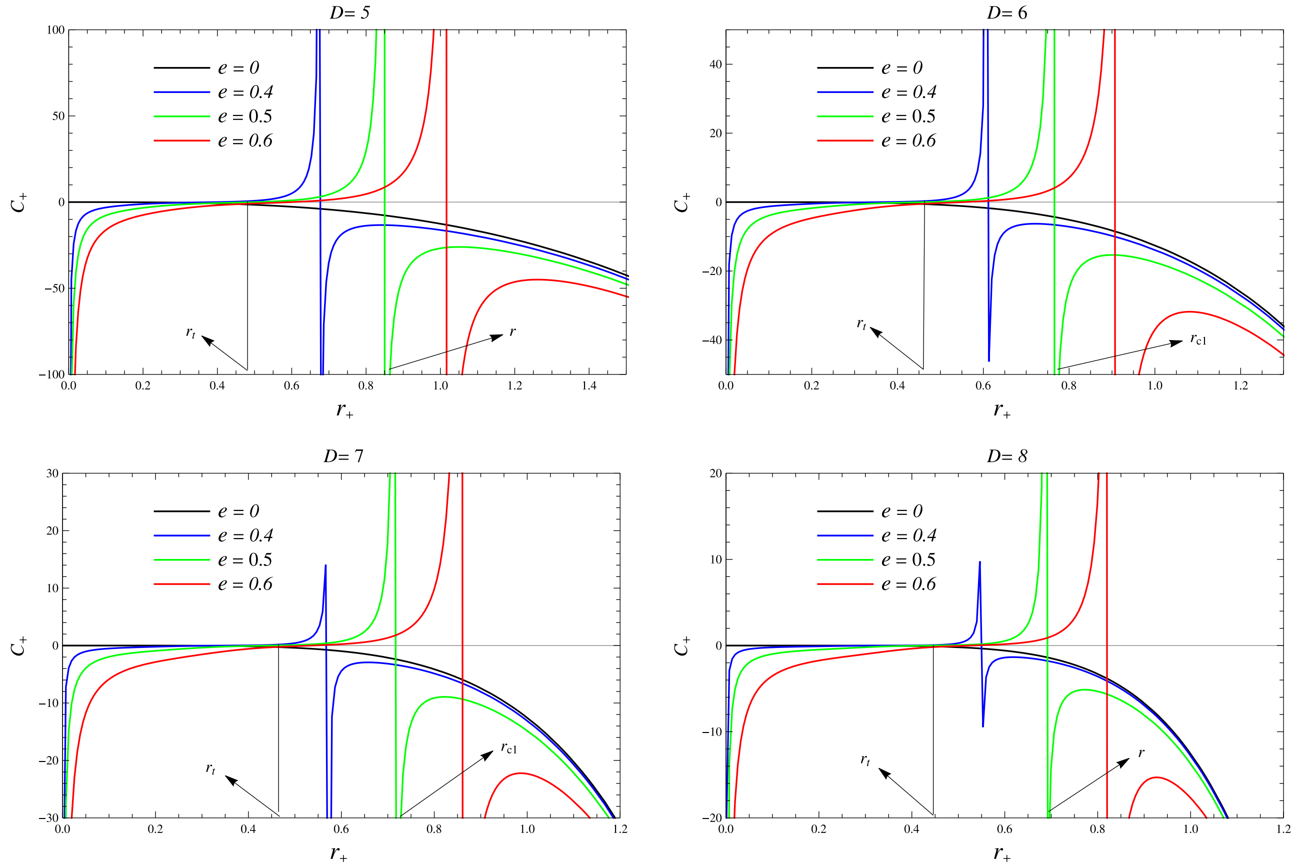

Fig. 7. Hayward black holes specific heat C_+ vs. horizon radius r_+ in various dimensions $D = 5$, 6, 7, and 8 for different values of e.

Table 3
The state and stability of Hayward EGB-AdS black holes with horizon radius r_+.

Region	State	Stability
$r_+ < r_{t1}$	Very small	Unstable
$r_{t1} < r_+ < r_+^c$	Small	Stable
$r_+^c < r_+ < r_{t2}$	Intermediate	Unstable
$r_+ > r_{t2}$	Large	Stable

heat capacity of EGB-AdS black holes, which reads [26,27]

$$C_+^{EGB-AdS} = \frac{(D-2)(D-3)V_{D-2}}{\beta_1} r_+^{D-4} \left[(r_+^2 + 2\tilde{\alpha})^2 (r_+^2 + \frac{D-5}{D-3}\tilde{\alpha} + \frac{D-1}{(D-3)l^2} r_+^4) \right], \tag{42}$$

with

$$\beta_1 = 4\left[\left(\frac{D-1}{l^2} r_+^2 - D + 3 \right) r_+^4 + \left(\frac{6(D-1)}{l^2} r_+^4 - (D-9) r_+^2 \right) \tilde{\alpha} - 2(D-5)\tilde{\alpha}^2 \right]$$

Note that the magnetic charge factor (e) and cosmological constant ($1/l^2$) in Eq. (41) modify the Gauss–Bonnet black hole specific heat [39], and taking the limit ($e = 0$, $1/l^2 = 0$), we recover it. The Gauss–Bonnet black holes specific heat reads [26,27],

$$C_+^{EGB} = \frac{(D-2)(D-3)V_{D-2}}{\beta_2} r_+^{D-4} \left[(r_+^2 + 2\tilde{\alpha})^2 r_+^2 + \frac{D-5}{D-3}(r_+^2 + 2\tilde{\alpha})^2 \tilde{\alpha} \right], \tag{43}$$

with

$$\beta_2 = 4\left[(-D+3) r_+^4 - (D-9) r_+^2 \tilde{\alpha} - 2(D-5)\tilde{\alpha}^2 \right]$$

In the limit ($\alpha \to 0$, $1/l^2 = 0$), we recover D-dimensional Hayward black holes specific heat as given below

$$C_+^H = \frac{(D-2)(D-3)V_{D-2}}{\beta_3} r_+^D \left[(1 + \frac{e^{D-1}}{r_+^{D-1}})^2 (1 - \frac{2}{D-3} \frac{e^{D-1}}{r_+^{D-1}}) \right], \tag{44}$$

with

$$\beta_3 = 4\left[2(\frac{e^{D-1}}{r_+^{D-1}})^2 + (D^2 - 3D + 6) r_+^2 \frac{e^{D-1}}{r_+^{D-1}} - (D-3) r_+^2 \right].$$

The behavior is depicted in Fig. 7, which also shows the phase transition confirming the instability of Schwarzschild–Tangherlini black holes [26]. For ($\alpha \to 0$, $1/l^2 = 0$) and magnetic charge ($e = 0$), we get the specific heat for Schwarzschild–Tangherlini black holes [26,27]

$$C_+^{ST} = -\frac{(D-2)V_{D-2}}{4} r_+^{D-2}. \tag{45}$$

We have discussed the condition for the local thermodynamical stability, which is related to the sign of heat capacity. Now, we are going to examine the global stability of black hole via Gibb's free energy, the reason for this is that even if the black hole is thermodynamically stable, it could be globally unstable or vice-versa. The Gibb's free energy of black hole can be defined as [36,42]

$$F_+ = M_+ - T_+ S_+ \tag{46}$$

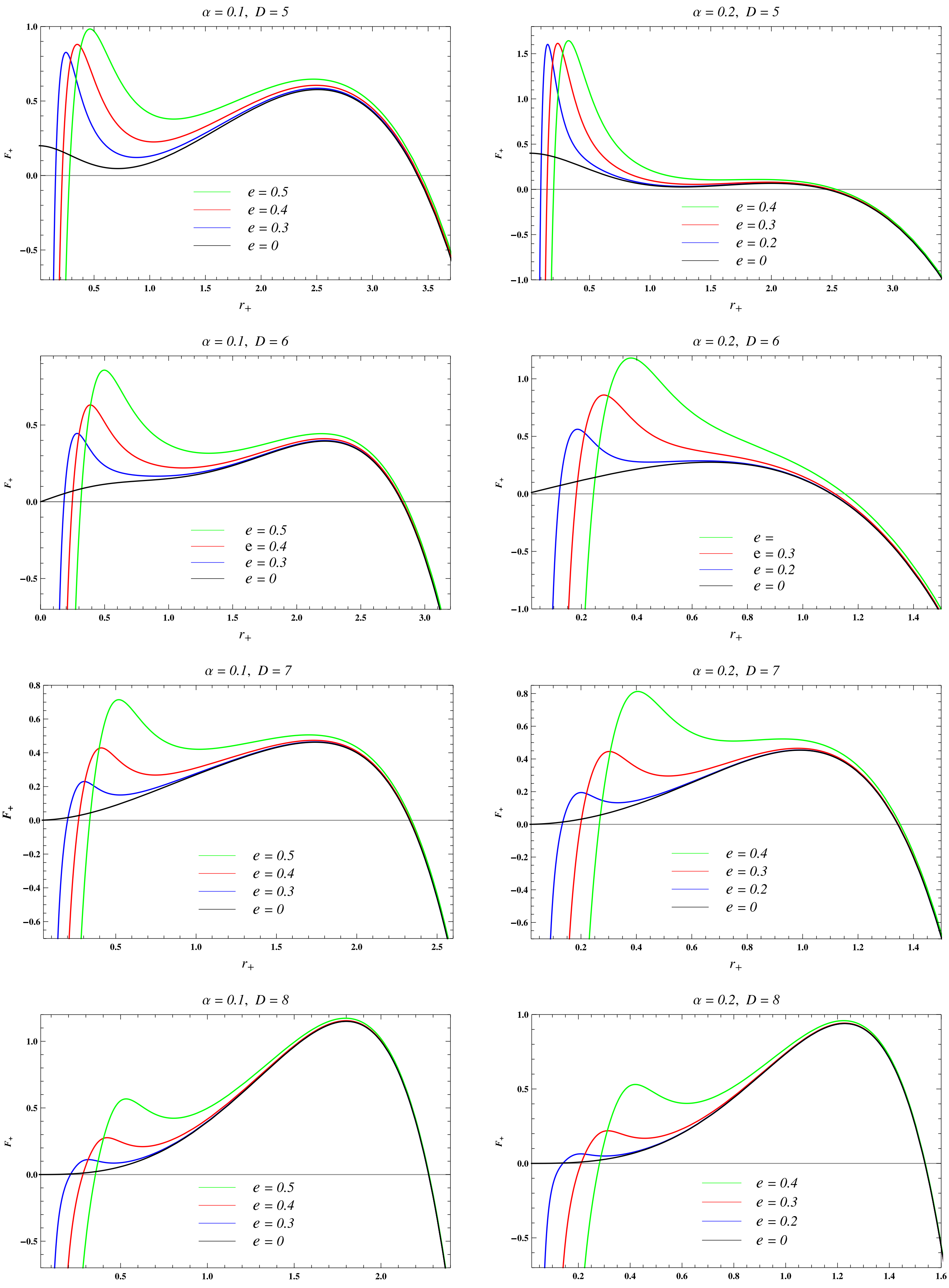

Fig. 8. Hayward EGB-AdS black holes Gibb's free energy F_+ vs. horizon radius (r_+) in the dimensions $D = 5$, 6, 7, and 8 (top to bottom) for different values of e with $e = 0$ corresponds to EGB-AdS black holes.

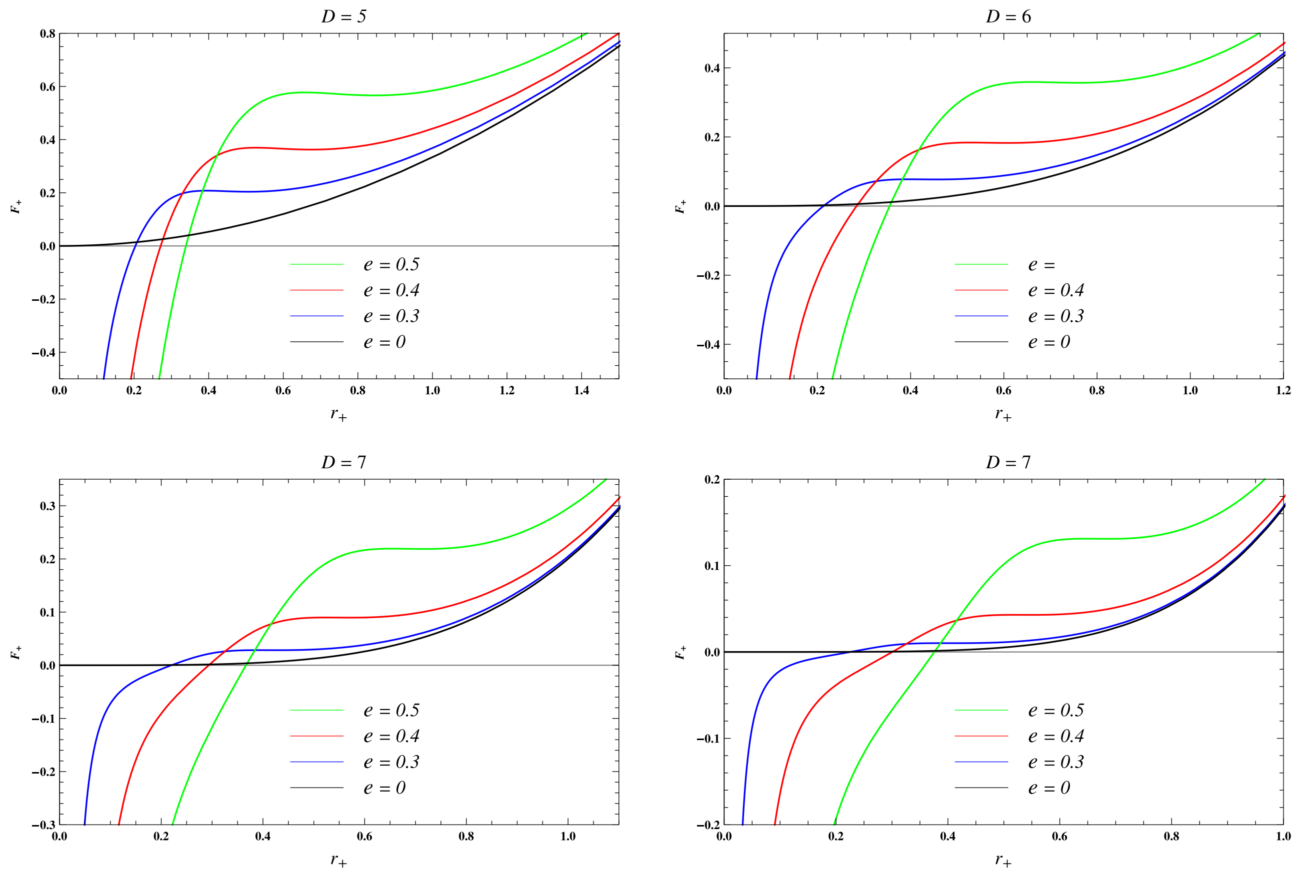

Fig. 9. Hayward black holes Gibb's free energy F_+ vs. horizon radius (r_+) in the dimensions $D = 5$, 6, 7, and 8 for different values of e with $e = 0$ corresponds to Schwarzschild–Tangherlini black holes.

Substituting Eqs. (27) and (32) in Eq. (46), we get the expression for free energy of Hayward EGB-AdS black holes, which reads

$$F_+ = \frac{V_{D-2}r_+^{D-5}}{16\pi(D-4)(r_+^2+2\tilde{\alpha})}\Big[(D-4)r_+^4\Big(1-\frac{r_+^2}{l^2}\Big)-\frac{6(D-2)\tilde{\alpha}r_+^4}{l^2} + (D-8)\tilde{\alpha}r_+^2+2(D-2)\tilde{\alpha}^2+ +A\frac{e^{D-1}}{r_+^{D-1}}-B\Big(\frac{e^{D-1}}{r_+^{D-1}}\Big)^2\Big] \tag{47}$$

where

$$A = \frac{1}{3}\Big[\,(D-2)(D-4)(3r_+^2+2\tilde{\alpha})\big((D-3)r_+^2+(D-5)\tilde{\alpha}\big) + 6(r_+^2+2\tilde{\alpha})\Big((D-1)(D-4)r_+^2+(D-2)^2\tilde{\alpha} + (D-2)(D-4)\frac{r_+^4}{l^2}\Big)\,\Big]$$

$$B = \frac{1}{3}\big[2(D-2)(D-4)(3r_+^4+8r_+^2\tilde{\alpha}+4\tilde{\alpha}^2)\big] \tag{48}$$

The sign of Gibb's free energy tells about the global stability of the black holes [22]. We know that negative free energy ($F_+ < 0$) signifies the global stability of the black holes, whereas the positivity of the free energy ($F_+ > 0$) confirms that the black holes are globally unstable [22]. The plot for free energy with a horizon radius (r_+) in various dimensions has been shown in Fig. 8. From Fig. 8, it is important to note that the black holes with very small and large horizon radius r_+ are globally stable, but the intermediate black holes are globally unstable. But, on the other hand, Hayward black holes are globally stable only for very small horizon radius r_+ and Schwarzschild–Tangherlini black holes are globally unstable (see Fig. 9). The behavior of Gibb's free energy of EGB-AdS black in various dimensions, for different values of $\tilde{\alpha}/l^2$, has been shown in Fig. 7, which is confirming that only the large EGB-AdS black holes are globally stable [22]. By making magnetic charge $e = 0$ in Eq. (52), one recovers the free energy for EGB-AdS black holes [22,36]

$$F_+^{EGB-AdS} = \frac{V_{D-2}r_+^{D-5}}{16\pi(D-4)(r_+^2+2\tilde{\alpha})}\Big[(D-4)r_+^4\Big(1-\frac{r_+^2}{l^2}\Big)-\frac{6(D-2)\tilde{\alpha}r_+^4}{l^2} + (D-8)\tilde{\alpha}r_+^2+2(D-2)\tilde{\alpha}^2+\Big] \tag{49}$$

which reduces to the free energy of EGB black holes [27], for $1/l^2 = 0$

$$F_+^{EGB} = \frac{V_{D-2}r_+^{D-5}}{16\pi(D-4)(r_+^2+2\tilde{\alpha})}\Big[(D-4)r_+^4+(D-8)r_+^2\tilde{\alpha}+2(D-2)\tilde{\alpha}^2\Big] \tag{50}$$

By keeping $\alpha \to 0$, $1/l^2 = 0$, we obtain the expression for free energy of D-dimensional Hayward black holes

$$F_+^{H} = \frac{V_{D-2}r_+^{D-5}}{16\pi(D-4)}\Big[(D-4)r_+^2+(D-4)(D^2-3D+4)\frac{e^{D-1}}{r_+^{D-3}} -2(D-2)(D-4)\Big(\frac{e^{D-1}}{r_+^{D-2}}\Big)^2\Big] \tag{51}$$

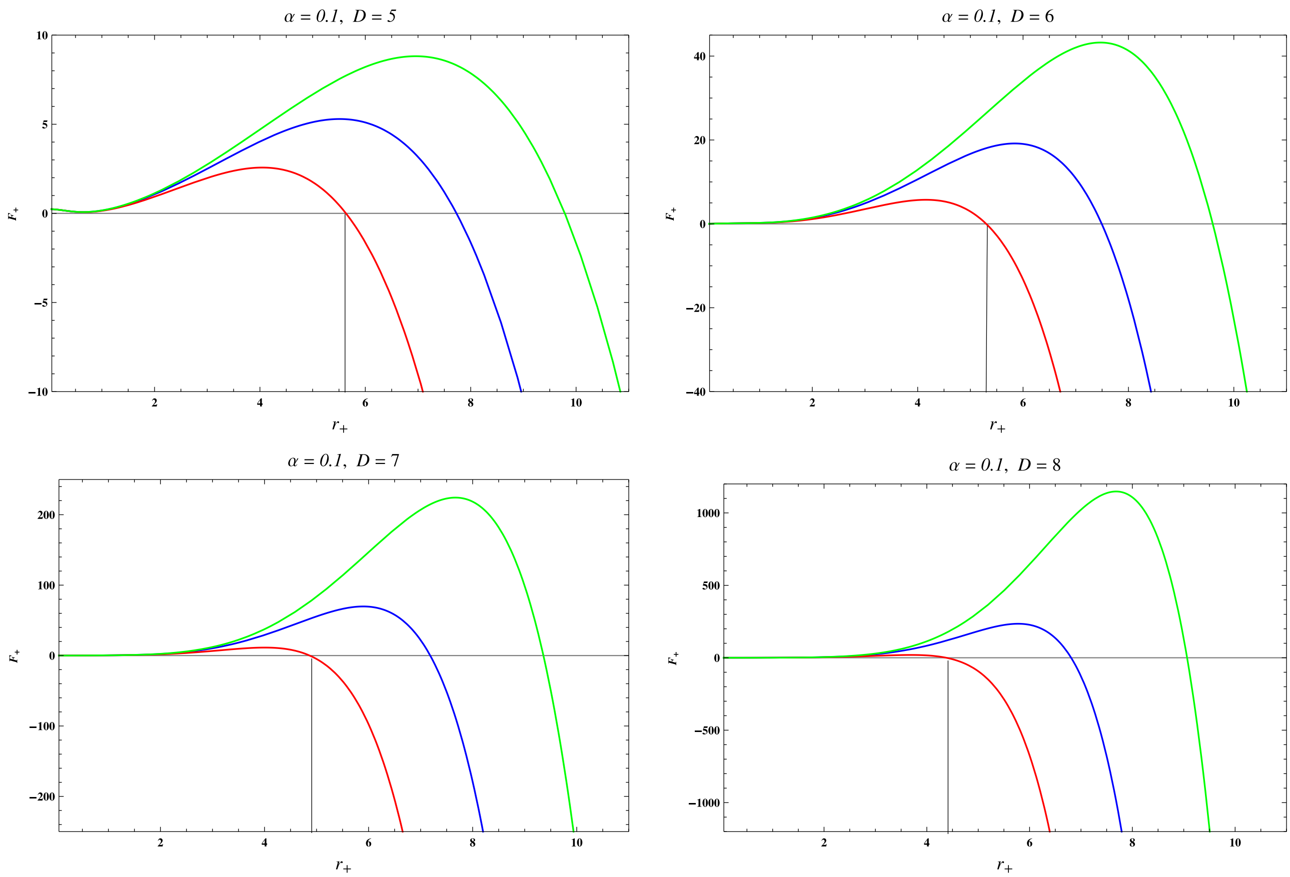

Fig. 10. EGB-AdS black holes Gibb's free energy F_+ vs. horizon radius (r_+) in various dimensions $D = 5$, 6, 7 and 8. The three curves from top to bottom correspond, respectively, to $l^2 = 100, 64$ and 36 [22].

which further goes to the free energy of Schwarzschild -Tangherlini black holes, in the limit $e = 0$

$$F_+^{ST} = \frac{V_{D-2} r_+^{D-3}}{16\pi} \tag{52}$$

The localized late stage of black hole undergoing the Hawking evaporation is termed as black hole remnant. The study of the black hole remnant becomes important given that it can be a candidate that can be used as the source for dark matter [43]. By using the relation, $f'(r)|_{r=r_E} = 0$, one can calculate the remnant size or the degenerate horizon radius ($r_\pm = r_E$) of extremal Hayward EGB-AdS black holes. We analyze the emitted feature of Hayward EGB-AdS black holes via the plots of the metric function (17) vs. radius in Fig. 11. The numerical results of black hole remnant mass μ' and remnant radius r_E has been tabulated in Tables 4 and 5. It is important to note that there exists a lower bound on mass, μ'_0, such that, $\mu' = (<)\ \mu'_0$ corresponds to extremal (no) black hole.

4. Concluding remarks

We consider, in arbitrary D-dimensions, quadratic corrections to Einstein–Hilbert action described by the Gauss–Bonnet term coupled to nonlinear electrodynamics and find the Hayward-charged black hole solutions with anti-de Sitter (AdS) asymptotics, of interest in the context AdS/CFT. Thus, we have presented exact D-dimensional Hayward-like black holes in Einstein–Gauss–Bonnet gravity with a negative cosmological constant, thereby generalizing Boulware–Deser black holes which are included as a special case ($e = 0$, $l^2 \to \infty$). The Hayward-EGB-AdS black holes are characterized by analyzing horizons, which at most could be two, viz. inner Cauchy and outer event horizons. In turn, we have analyzed the horizon thermodynamical properties and phase structure of these AdS black holes. Despite complicated solutions, we obtain the exact expression for the thermodynamical quantities like the black hole mass, Hawking temperature, entropy and free energy at event horizon r_+ and in turn, we also analyze the thermodynamical stability of the black holes by studying the specific heat. The entropy (37) of the black holes is modified due to the magnetic charge e and the GB parameter α, and area law $S = A/4$ is no longer valid. The phase transition is detectable by the divergence of the heat capacity (C_+) at a critical radius r_c (changes with e, α, l^2 and dimensions D), such that the black hole is stable in the region viz: $r_{t1} < r_+ < r_C$ and $r_+ > r_{t2}$ with positive heat capacity ($C_+ > 0$), on the other hand the heat capacity is negative ($C_+ < 0$), when $r_+ < r_{t1}$ and $r_c < r_+ < r_{t2}$, indicating the instability of black holes. Interestingly, the smaller and larger Hayward EGB-AdS black holes are stable with ($F_+ < 0$) (Fig. 8). In contrast only smaller Hayward and only larger EGB-AdS black holes ($r_+ \gtrsim 5.6$ in 5D) are globally stable with negative free energy (Figs. 9 and 10). Finally, Hayward EGB-AdS black holes do not completely evaporate, but halts into a stable remnant with vanishing temperature, degenerate horizons and positive heat capacity $C_+ > 0$. The black hole remnant size and mass for different values of the black hole parameters are also given.

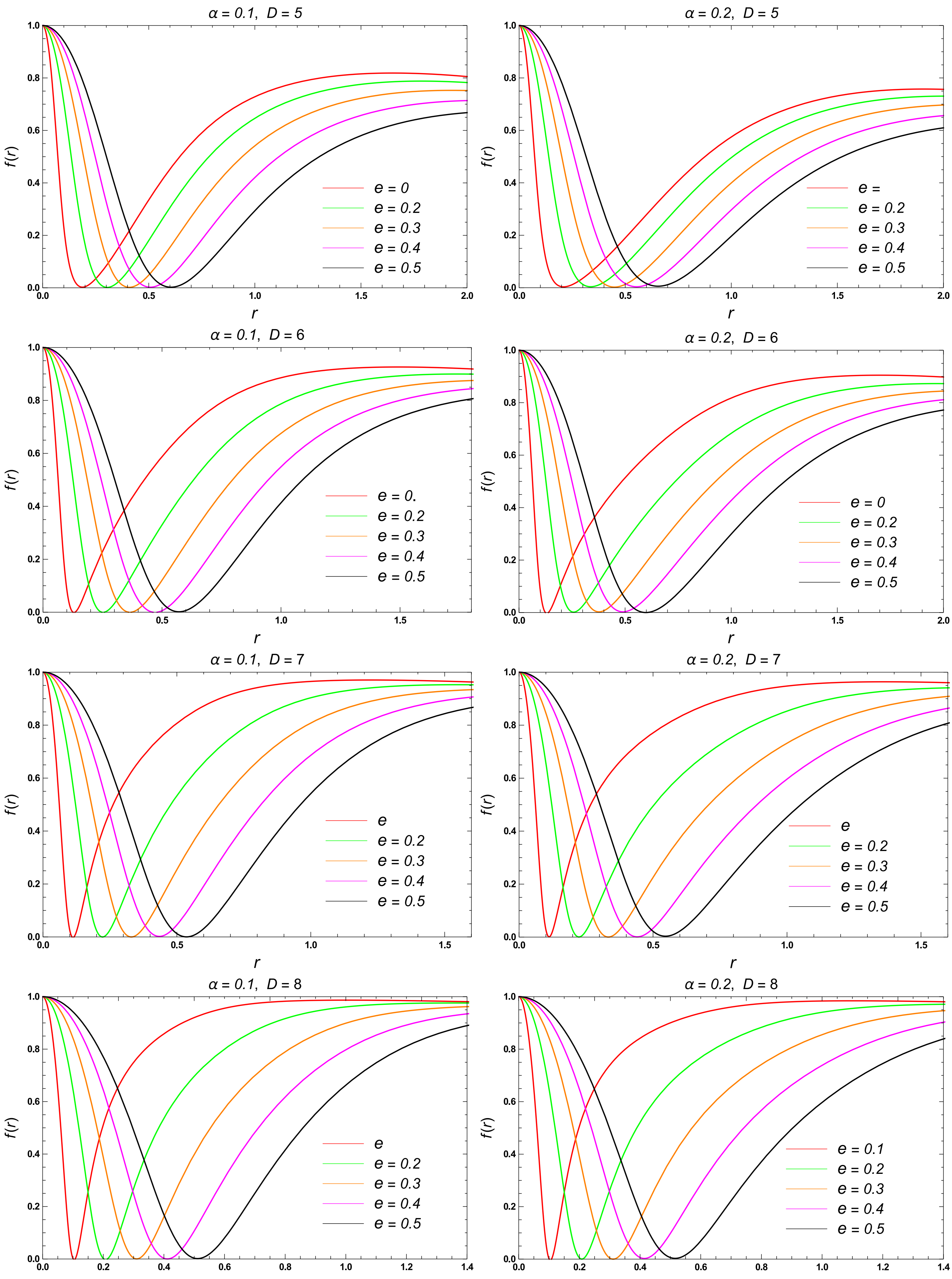

Fig. 11. Hayward EGB-AdS black holes metric function $f(r)$ vs. r in various dimensions $D = 5$, 6, 7, and 8 (top to bottom) for different values of e.

Table 4
The remnant radius (r_0) and the remnant mass term (μ'_0) for different values of parameter (e) for Gauss–Bonnet coupling parameter ($\alpha = 0.1$).

Magnetic charge	$D=5$		$D=6$		$D=7$		$D=8$	
e	r_0	μ'_0	r_0	μ'_0	r_0	μ'_0	r_0	μ'_0
0.1	0.181	0.253	0.133	0.102	0.115	0.023	0.106	0.004
0.2	0.307	0.346	0.255	0.220	0.230	0.094	0.215	0.032
0.3	0.418	0.471	0.376	0.368	0.337	0.223	0.315	0.112
0.4	0.508	0.629	0.479	0.558	0.337	0.420	0.421	0.275
0.5	0.610	0.821	0.589	0.797	0.540	0.708	0.515	0.559

Table 5
The remnant radius (r_0) and the remnant mass term (μ'_0) for different values of parameter (e) for Gauss–Bonnet coupling parameter ($\alpha = 0.2$).

Magnetic charge	$D=5$		$D=6$		$D=7$		$D=8$	
e	r_0	μ'_0	r_0	μ'_0	r_0	μ'_0	r_0	μ'_0
0.1	0.214	0.464	0.136	0.202	0.112	0.045	0.106	0.008
0.2	0.344	0.573	0.263	0.417	0.226	0.185	0.215	0.064
0.3	0.459	0.717	0.373	0.664	0.334	0.427	0.315	0.219
0.4	0.565	0.890	0.491	0.956	0.442	0.784	0.415	0.526
0.5	0.667	1.093	0.610	1.310	0.553	1.270	0.521	1.050

Finally, we recovered all results of EGB-AdS/EGB black holes in the limits $e = 0/e = \Lambda = 0$ and that of the general relativity when $\alpha \to 0$. It would be interesting in this case to analyze the effective thermodynamics and also investigate these models in the general Lovelock gravity.

Declaration of competing interest

The authors declare that they have no known competing financial interests or personal relationships that could have appeared to influence the work reported in this paper.

Acknowledgments

S.G.G. would like to thanks DST INDO-SA bilateral project DST/INT/South Africa/P06/2016 and also to IUCAA, Pune for the hospitality while this work was being done.

References

[1] J.A. Wheeler, in: C. DeWitt, B. DeWitt (Eds.), Relativity, Groups, and Topology, Gordon and Breach, New York, 1964, p. 315.
[2] S. Ansoldi, arXiv:0802.0330 [gr-qc].
[3] J. Bardeen, Proceedings of GR5, Tiflis, U.S.S.R., 1968.
[4] E. Ayon-Beato, A. Garcia, Phys. Lett. B 493 (2000) 149.
[5] I. Dymnikova, Gen. Relativity Gravitation 24 (1992) 235;
I. Dymnikova, Classical Quantum Gravity 21 (2004) 4417;
K.A. Bronnikov, Phys. Rev. D 63 (2001) 044005.
[6] L. Xiang, Y. Ling, Y.G. Shen, Internat. J. Modern Phys. D 22 (2013) 1342016.
[7] L. Balart, E.C. Vagenas, Phys. Lett. B 730 (2014) 14.
[8] L. Balart, E.C. Vagenas, Phys. Rev. D 90 (2014) 124045.
[9] J.C.S. Neves, A. Saa, Phys. Lett. B 734 (2014) 44.
[10] S. Fernando, Internat. J. Modern Phys. D 26 (2016) 1750071.
[11] S.A. Hayward, Phys. Rev. Lett. 96 (2006) 031103.
[12] R. Kumar, S.G. Ghosh, A. Wang, Phys. Rev. D 100 (12) (2019) 124024.
[13] S.H. Mehdipour, M.H. Ahmadi, Nuclear Phys. B 296 (2018) 49–69.
[14] V.P. Frolov, Phys. Rev. D 94 (2016) 104056; EPJ Web Conf. 168 (2018) 01001.
[15] S.S. Zhao, Y. Xie, Eur. Phys. J. C 77 (2017) 272;
S.G. Ghosh, S.D. Maharaj, Eur. Phys. J. C 75 (2015) 7;
S.G. Ghosh, Eur. Phys. J. C 75 (2015) 532;
S.G. Ghosh, D.V. Singh, S.D. Maharaj, Phys. Rev. D 97 (2018) 104050.
[16] N. Seiberg, E. Witten, J. High Energy Phys. 032 (1999) 9909;
E.S. Fradkin, A. Tseytlin, Phys. Lett. B 163 (1985) 123;
A. Tseytlin, Nucl. Phys. B 276 (1985) 391.
[17] D.J. Gross, E. Witten, Nuclear Phys. B 277 (1986) 1.
[18] D.G. Boulware, S. Deser, Phys. Rev. Lett. 55 (1985) 2656;
Gross, J.H. Sloan, Nucl. Phys. B 291 (1987) 41.
[19] D. Wiltshire, Phys. Rev. D 38 (1988) 2445.
[20] I.P. Neupane, Phys. Rev. D 69 (2004) 084011;
I.P. Neupane, Phys. Rev. D 67 (2003) 061501.
[21] T. Torii, H. Maeda, Phys. Rev. D 71 (2005) 124002.
[22] Y.M. Cho, I.P. Neupane, Phys. Rev. D 66 (2002) 024044.
[23] D. Lovelock, J. Math. Phys. (N.Y.) 12 (1971) 498.
[24] M.H. Dehghani, S.H. Hendi, Internat. J. Modern Phys. D 16 (2007) 1829.
[25] D. Kastor, R.B. Mann, J. High Energy Phys. 04 (2006) 048.
[26] S.G. Ghosh, U. Papnoi, S.D. Maharaj, Phys. Rev. D 90 (2014) 044068.
[27] A. Kumar, D.V. Singh, S.G. Ghosh, Eur. Phys. J. C 79 (2019) 275.
[28] S.H. Hendi, S. Panahiyan, B. Eslam Panah, J. High Energy Phys. 01 (2016) 129.
[29] S. Fernando, Internat. J. Modern Phys. D 26 (2017) 1750071.
[30] B. Zwiebach, Phys. Lett. B 156 (1985) 315.
[31] G. Kunstatter, H. Maeda, Classical Quantum Gravity 31 (2014) 115009.
[32] R.C. Myers, J.Z. Simon, Phys. Rev. D 38 (1988) 2434.
[33] R. Ruffini, J.A. Wheeler, Phys. Today 24 (12) (1971) 30.
[34] C.W. Misner, K.S. Thorne, J.A. Wheeler, Gravitation (1973).
[35] S.W. Hawking, D.N. Page, Comm. Math. Phys. 87 (1983) 577.
[36] R.G. Cai, Phys. Rev. D 65 (2002) 084014.
[37] P. Kanti, Lecture Notes in Phys. 769 (2009) 387, 423.
[38] F.R. Tangherlini, Nuovo Cimento 27 (1963) 636.
[39] C. Sahabandu, P. Suranyi, C. Vaz, L.C.R. Wijewardhana, Phys. Rev. D 73 (2006) 044009.
[40] M. Cvetic, S. Nojiri, S.D. Odintsov, Nuclear Phys. B 628 (2002) 295.
[41] J.D. Bekenstein, Phys. Rev. D 7 (1973) 2333.
[42] E. Herscovich, M.G. Richarte, Phys. Lett. B 689 (2010) 192–200.
[43] J.H. MacGibbon, Nature 329 (1987) 308.